We are IntechOpen,
the world's leading publisher of
Open Access books
Built by scientists, for scientists

6,900
Open access books available

186,000
International authors and editors

200M
Downloads

154
Countries delivered to

Our authors are among the

TOP 1%
most cited scientists

12.2%
Contributors from top 500 universities

CLARIVATE ANALYTICS
BOOK CITATION INDEX
INDEXED

WEB OF SCIENCE™

Selection of our books indexed in the Book Citation Index
in Web of Science™ Core Collection (BKCI)

Interested in publishing with us?
Contact book.department@intechopen.com

Numbers displayed above are based on latest data collected.
For more information visit www.intechopen.com

Impact of Atmospheric Variability on Soil Moisture-Precipitation Coupling

Jiangfeng Wei[1], Paul A. Dirmeyer[1], Zhichang Guo[1] and Li Zhang[2]

[1]Center for Ocean-Land-Atmosphere Studies,
Institute of Global Environment and Society,
Calverton, Maryland,
[2]NOAA/NWS/NCEP/Climate Prediction Center,
Camp Springs, Maryland
USA

1. Introduction

It is now well-established that the chaotic nature of the atmosphere severely limits the predictability of weather, while the slowly varying sea surface temperature (SST) and land surface states can enhance the predictability of atmospheric variations through surface-atmosphere interactions or by providing a boundary condition (e.g., Shukla 1993, 1998; Shukla et al. 2000; Graham et al. 1994; Koster et al. 2000; Dirmeyer et al. 2003; Quan et al. 2004). Among them, the influence of ocean is more important on a global scale because it covers twice as much surface area as land and is a much larger heat and energy reservoir. But the impact of ocean may not be dominant over land, especially the mid-latitude land (Koster and Suarez 1995).

The Global Land-Atmosphere Coupling Experiment (GLACE) (Koster et al., 2004, 2006) builds a framework to objectively estimate the potential contribution of land states to atmospheric predictability (called land-atmosphere coupling strength) in numerical weather and climate models. By averaging the estimated land-atmosphere coupling strength from 12 models participating in GLACE, an ensemble average coupling strength is obtained. However, the coupling strength varies widely among models. The discrepancy is certainly related to differences in the parameterization of processes and their complex interactions, from soil hydrology, vegetation physiology, to boundary layer, cloud and precipitation processes. It is difficult to determine what causes the relatively strong or weak coupling strengths seen in individual models.

Some studies have identified the impact of soil moisture on evapotranspiration (ET) (denoted SM→ET) and the impact of ET on precipitation (denoted ET→P) as two key factors for land-atmosphere coupling (Guo et al. 2006 (hereafter GUO06); Dirmeyer et al. 2010). For soil moisture to have a strong impact on precipitation, both SM→ET and ET→P need to be strong. This usually happens in transitional zones between wet and dry climates (Dirmeyer 2006). In addition to the mean climate state, does the climate variability have some impact on land-atmosphere coupling? A theoretical study found that the strength of the external forcing can affect the coupling strength and the location of coupling hot spots (Wei et al. 2006). Even less is known about how the land-atmosphere coupling is related to the

different timescales of climate variability. The intraseasonal variability of precipitation has a strong influence on the soil moisture variability (Wei et al. 2008), but little has been done on the connection between this variability and land-atmosphere coupling.

In this paper, we reviewed our recent work on the impact of atmospheric variability on soil moisture-precipitation coupling, mainly from Wei et al. (2010b) and Wei and Dirmeyer (2010). The paper first presents our results of GLACE-type experiments with two different Atmospheric General Circulation Models (AGCMs) coupled to three different land surface schemes (LSSs). The large-scale connections between precipitation predictability, land-atmosphere coupling strength, and climate variability are examined, and the roles of different model components and different action processes in land-atmosphere coupling are investigated. Based on the analyses, the model estimated land-atmosphere coupling strength can be calibrated to account for errors in the simulation of precipitation variability, a quantity that is observable in the large scale and found to be closely related to the coupling strength.

2. Models and experiments

The two AGCMs are a recent version of the Center for Ocean-Land-Atmosphere Studies (COLA) AGCM (Misra et al., 2007; Kinter et al., 1997) and a recent operational version of the National Center for Environmental Prediction (NCEP) Global Forecast System (GFS) model. The COLA AGCM is configured with 28 vertical sigma levels, while GFS is configured with 64 vertical sigma levels. They both have a spectral triangular truncation of 62 waves (T62) in the horizontal resolution (approximately 1.9º grid). The three LSSs are: the latest version of the COLA simplified Simple Biosphere model (SSiB) (based on Xue et al., 1991; Dirmeyer and Zeng 1999), the version 3.5 of the Community Land Model (CLM3.5) (Oleson et al., 2004, 2008), and a recent version of the Noah land model (Ek et al., 2003). Wei et al. (2010a) gave a brief introduction of the recent changes of these LSSs. There are many specific differences among these LSSs in the parameterization of particular processes. In addition, the three LSSs have different numbers of soil layers and soil depths, and each uses its own soil and vegetation data sets.

Two experiments are preformed in this study:

1. GLACE-type experiments are performed with each of the six different model configurations. Detailed descriptions of the experiments and the indexes are in the Appendix. The ensemble W is the same as the standard GLACE experiment, while in ensemble S the soil moisture in all the soil layers is replaced, instead of only the subsurface soil moisture, in order to make the results from different LSSs comparable (see Appendix).

2. As the two AGCMs have different precipitation variabilities (shown below), which may lead to different soil moisture variabilities, the purpose of experiment (2) is to investigate the respective impacts of atmospheric variability and soil moisture variability on land-atmosphere coupling. Modified GLACE-type experiments are performed with COLA-SSiB and GFS-SSiB. The difference from experiment (1) is that, in the S runs, all members of the COLA-SSiB ensemble reads the same soil moisture from one W run of GFS-SSiB, while all members of the GFS-SSiB ensemble reads the same soil moisture from one W run of COLA-SSiB. The W ensembles are the same as in experiment (1). Although both from SSiB, the soil moisture climatologies of the two model configurations will be somewhat different, but this effect should be small compared to that of the dramatically different variabilities driven by precipitation.

3. Results from GLACE-type experiments

Fig. 1 shows the Ω_p values of total precipitation for ensembles W (16-member control experiment for June-July-August (JJA)) and S (soil wetness specified in all ensemble members from an arbitrarily chosen member of W) and their difference $\Omega_p(S) - \Omega_p(W)$ (see the appendix for complete definitions). The three indexes are generally higher when the LSSs are coupled to the COLA AGCM than to GFS, indicating that the difference in AGCM is the main reason for these differences. The impact of different LSSs, which can be seen from the varying spatial distributions of the indexes when coupled to the same AGCM, is secondary. Ω_p shows largely similar patterns for all the six model configurations, with the largest values in the tropical rain belt where the SST forcing has the strongest influence (Shukla 1998). The patterns of $\Omega_p(W)$ and $\Omega_p(S)$ are very similar, with large differences ($\Omega_p(S) - \Omega_p(W)$) mainly over the regions with common high values. This indicates that the land-atmosphere coupling strength may be strongly influenced by the external forcing. By "external", we mean the forcing is from outside of the land-atmosphere system, such as that from SST. The patterns of $\Omega_p(S) - \Omega_p(W)$ for different model configurations have much lower similarity than those of Ω_p (spatial correlations are 0-0.29 for $\Omega_p(S) - \Omega_p(W)$ and 0.43-0.71 for Ω_p). For both AGCMs, coupling to SSiB produces the strongest land-atmosphere coupling strength globally, while coupling to Noah produces the weakest. The differences seen should be mainly from the land models' different connections between soil moisture and surface fluxes, because they are coupled to the same AGCM.

4. A decomposed view of land-atmosphere coupling strength

As discussed above, the slowly varying boundary forcing may play an important role in the similarity of the precipitation time series in different ensemble members (magnitude of Ω_p). It is very likely that the "fingerprints" of these slow forcings also exist in the precipitation time series. An effective way to examine this is to decompose the time series by frequency bands. After ignoring the first 8 days of integration of each JJA to avoid possible problems associated with the initial shock to the model atmosphere, as in calculating Ω_p, there remain 84 days left for analysis. We performed a discrete Fourier transform (discussed in detail in Ruane and Roads (2007)) to decompose the daily time series into three frequency bands: fast synoptic (2-6 days), slow synoptic (6-20 days), and intraseasonal (20-84 days). The choice of these frequency bands is arbitrary; other comparable choices give similar results. Note that the time series may contain a portion of the seasonal cycle, but due to the length of the time series we refer the 20-84 days variation as intraseasonal.

Fig. 2 shows the variance percentages of precipitation in these three bands for model simulations and the observationally based Global Precipitation Climatology Project One-Degree Daily (GPCP-1DD) datasets (at 1°×1° resolution, from 1997-2009) (http://precip.gsfc.nasa.gov/gpcp_daily_comb.html; Huffman et al. 2001). For a specific AGCM, the three model configurations are very consistent in their variance distributions. However, compared to the GPCP-1DD data, all the model simulations underestimate the high-frequency (fast synoptic) variance and overestimate the low-frequency (intraseasonal) variance, especially over tropics and subtropics. Multi-year simulations of these models,
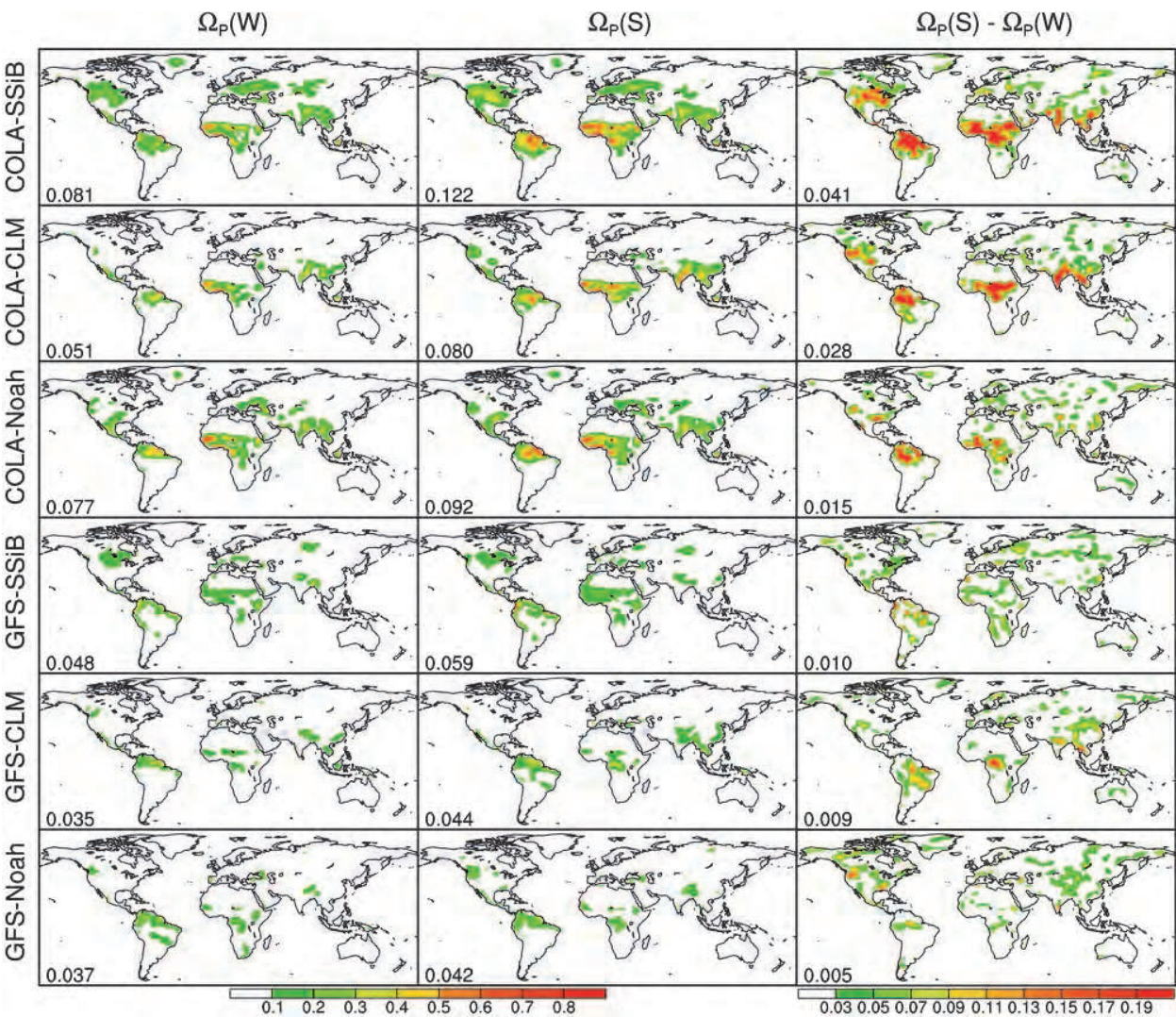
Fig. 1. The GLACE parameter Ω for precipitation from ensembles (left column) W and (middle column) S, and (right column) their difference. The six rows are for six different model configurations. The global mean (land only) value of each panel is shown at the left corner.

have similar variance percentage distributions as these GLACE-type simulations (not shown).

For theoretical white noise, the variance at each frequency is the same, so the variance percentages are determined by the widths of the frequency bands. Therefore, the variance percentages of the above three bands (from fast to slow) for white noise are: 69%, 21%, and 10%, respectively. Overall, both the model results and observations follow a red spectrum, with variance percentages less than white noise values at high frequencies and greater than white noise values at low frequencies.

In Fig. 2, the spatial correlations between $\Omega_p(W)$ and the percentage of intraseasonal variance (IV) are high (right column), but the correlations of $\Omega_p(W)$ with the other two frequency bands are negative (left two columns). Ensemble S (not shown) shows similar results as ensemble W. This demonstrates that regions with a larger percentage of IV tend to have a higher value of Ω_p, no matter whether soil moisture is interactive (W) or not (S).
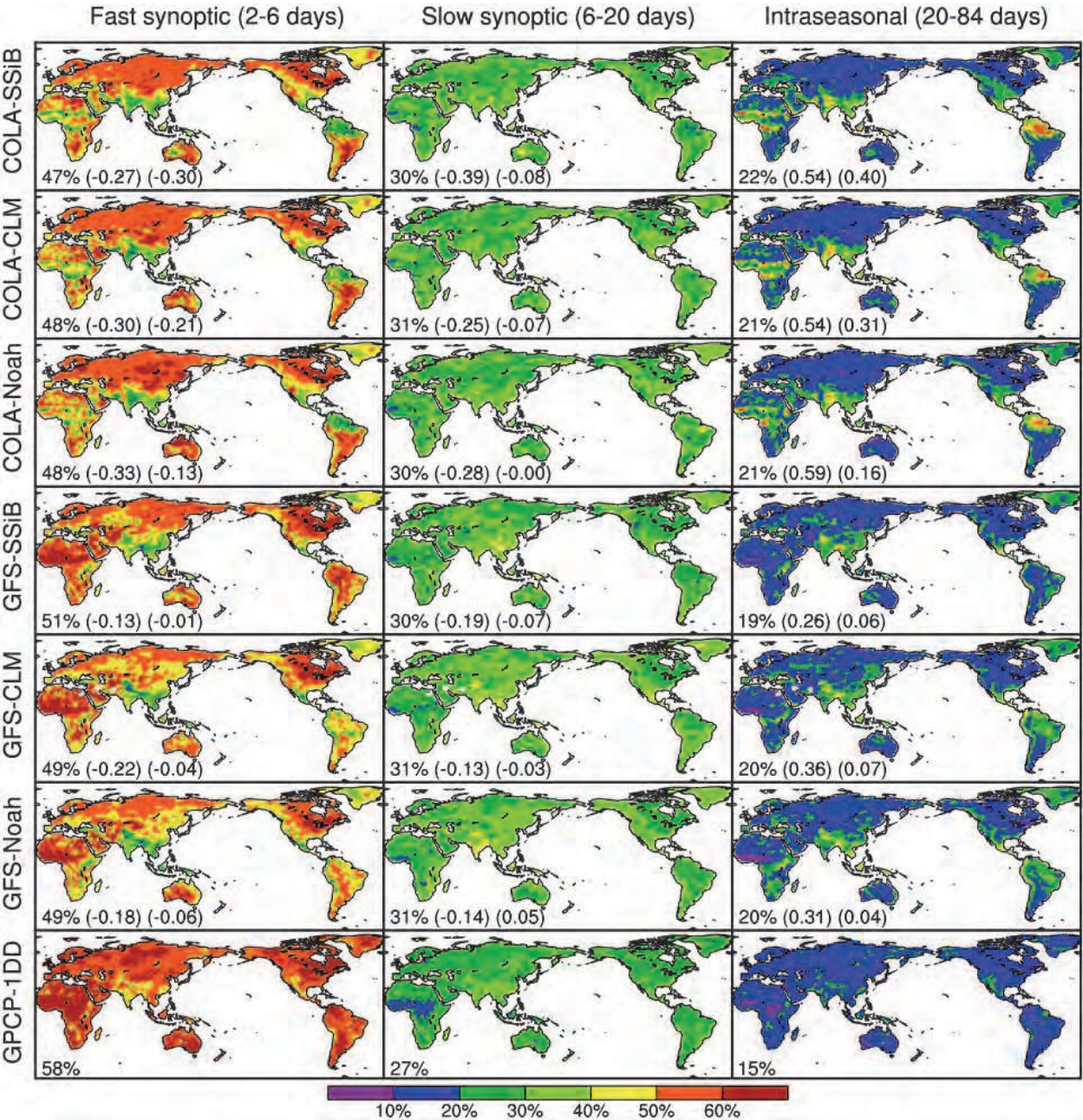
Fig. 2. The average variance percentages of JJA daily precipitation time series in three frequency bands: fast synoptic (2-6 days; left column), slow synoptic (6-20 days; middle column), and intraseasonal (20-84 days; right column). The top six rows are from six different model configurations (all from ensemble W; ensemble S has similar results), and the bottom row is from the observationally based dataset of GPCP-1DD. The value (or three values) at the left corner of each panel is the global mean percentage, (the spatial correlations of the variance percentage with $\Omega_p(W)$, and with $\Omega_p(S) - \Omega_p(W)$). The GPCP-1DD datasets are shown at 1°×1° grid; interpolating them to model grid does not affect the results.

This is not unexpected because, as we discussed above, most of the precipitation predictability (or Ω_p) is from the slowly varying boundary forcing. Regions with stronger boundary forcing may be constrained to show more low-frequency variation and the precipitation time series will be more similar in an ensemble (larger Ω_p). For ensemble S, the prescribed soil moisture is also one of the slow boundary forcings. However, compared to the ensemble without the constraint of this slow forcing (W), ensemble S does not show significant change in the global pattern of variance distribution (ensemble S does show overall less low-frequency variance and more high-frequency variance than ensemble W because of the lack of soil moisture interaction (Delworth and Manabe 1989)). These results show that different land models or land states do not matter much for the global pattern of precipitation variance distribution, which may be determined by other factors such as global climate (SST, radiation etc.) and the convection scheme. Ruane and Roads (2008) obtained similar results from a global assimilation system. They found that two different land models did not produce a noticeable difference in variance distribution of precipitation, but two different convection schemes can have significantly different effect. Wilcox and Donner (2007) also showed that the convection parameterization of a GCM can greatly impact the frequency distribution of rain rate, and their model with relaxed Arakawa-Schubert formulation of cumulus convection (also used in COLA AGCM) exhibit a strong bias toward excessive light rain events and too few heavy rain events.

The above shows that neither the land model nor soil moisture has a great impact on the global pattern of precipitation variability and predictability. However, their impact may be strong at regional scales. The difference $\Omega_p(S) - \Omega_p(W)$ shows the impact of soil moisture. It tries to remove the effects of the same strong external forcing on both S and W and highlight the role of soil moisture, although we understand that the effects of those forcing cannot be completely removed in a nonlinear system (more discussion on this aspect follows). The spatial correlations between percentage of IV and $\Omega_p(S) - \Omega_p(W)$ are also shown in Fig. 2 (as the last number in right column). They are generally weaker than the correlation with Ω_p, indicating that something other than the low-frequency external forcing is playing an important role in $\Omega_p(S) - \Omega_p(W)$. This should be the impact of soil moisture.

Wei et al. (2010b) demonstrates that the pattern of Ω_p and $\Omega_p(S) - \Omega_p(W)$ in Fig. 1 can be reproduced by using only the time series of intraseasonal precipitation variation (higher frequencies filtered out), and the time series of the other two frequency bands result in very weak values. This is because the intraseasonal component of precipitation, mostly caused by the same low-frequency external forcing, has high consistency among the ensemble members, while the high frequency component of precipitation, mostly from chaotic atmospheric dynamics, is generally incoherent among the ensemble members. This result indicates the importance of IV in the estimation of land-atmosphere coupling.

The overestimation of low-frequency variance shown in Fig. 2 is also consistent with the overestimation of precipitation persistence shown in Fig. 3. The lag-2-pentad autocorrelation of precipitation (ACR) shown here is also an indicator of the percentage of low-frequency precipitation variance, and it has similar spatial distributions as the percentage of IV but is much easier to calculate. More importantly, its spatial distributions are more similar to that of $\Omega_p(W)$ than the percentage of IV, as can be seen from the much higher spatial correlations (Fig. 3). This is probably because the percentage of IV only considers the variation at a certain frequency band (20-84 days here) but ACR considers the general

persistence and is not restricted by certain frequencies. It can also be seen in Fig. 3 that the precipitation variability of GFS is overall closer to that of GPCP data (Xie et al. 2003) than the COLA AGCM, which may affect the accuracy of the simulated land-atmosphere coupling. This will be discussed next.

This model bias has also been shown in some other studies and by comparing with other observational datasets. Although the observational datasets have uncertainties and errors, Sun et al. (2006) found that no matter what observational dataset is used, this model bias is relatively large compared to the uncertainties among observations. This bias of the models may be related to a well-known problem in AGCM parameterizations: premature triggering of convection so that precipitation falls too frequently but too light in intensity (Trenberth et al. 2003; Sun et al. 2006; Ruane and Roads 2007).

Fig. 3. The JJA lag-2-pentad autocorrelation (ACR) of pentad precipitation time series for (top six) different model configurations and (bottom) GPCP data. The model data are from 16 ensembles of W (sample size 16x16=256) , while the GPCP data are from16 years (1987-2002) to match the sample size of the models. Values larger than 0.12 are over 95% confidence level. Seasonal cycles are not removed in this calculation; removing them can lead to results with similar patterns but smaller amplitude.

5. Respective role of land and atmosphere in soil moisture-precipitation coupling

The above has shown that the low-frequency precipitation variability has an indirect but important connection to the computed land-atmosphere coupling. More low-frequency precipitation variability in the model can lead to higher precipitation predictability (Ω_p) and stronger land-atmosphere coupling ($\Omega_p(S) - \Omega_p(W)$). Therefore, there are three different processes involved: SM→ET, ET→P, and precipitation variability. What is the relationship among them? GUO06 separated SM→ET and ET→P based on a post hoc analysis, but they did not explicitly separate the role of soil moisture and atmosphere because ET is strongly affected by precipitation and radiation; the variability of ET is an approximation of low-frequency atmospheric variability. Thus SM→ET inevitably includes some information from atmosphere, including precipitation variability. The multi-model coupling approach provides a unique tool to estimate the respective impacts of the AGCMs and LSSs on the coupling, and only by this approach can the role of atmosphere and land be completely separated.

Although the above experiment shows the dominant role of the AGCMs in land-atmosphere coupling, it is still uncertain what are the roles of land and atmosphere in the coupling because the characteristics of the AGCMs may also affect land and its response. How important is the land response compared to the characteristics of the atmosphere (including atmospheric variability, sensitivity of precipitation to ET, etc.)? As the precipitation has more persistence in the COLA AGCM than in GFS, this attribute of precipitation variability is stored in the soil moisture, with more sustained soil states when the LSSs are coupled to the COLA AGCM than coupled to GFS (not shown). In order to investigate the impact of soil moisture variability on the coupling, in experiment (2) we exchange the prescribed soil moistures for COLA-SSiB and GFS-SSiB in ensemble S. This forces the models to see different soil moisture variabilities from their original S ensembles, and there is no change to the W ensembles. The resulting impacts on precipitation predictability (or coupling strengths) are shown in Fig. 4 (denoted $\Omega_P(S') - \Omega_P(W)$). It can be seen that, compared to the original coupling strength in Fig. 1, the modified coupling strength are overall weaker for COLA-SSiB and stronger for GFS-SSiB, but COLA-SSiB still has much stronger coupling strength than GFS-SSiB. This indicates that the impact of soil moisture variability may have some impact on the land-atmosphere coupling, but the characteristics of the atmosphere appear to be more important, at least for the case here. Note that the above action processes may be model dependent and vary spatially, but it is important to know that the atmospheric variability may also impact the coupling strength indirectly through land. Therefore, the precipitation variability impacts soil moisture-precipitation coupling both directly in the atmosphere and indirect through land (Fig. 5). More low-frequency variability of soil moisture usually means more sustained dry and wet periods and stronger low-frequency evaporation variation, which can lead to a more robust precipitation response (higher predictability and coupling strength). The direct impact of precipitation variability on soil moisture-precipitation coupling has been discussed in section 4 and more discussion follows.

GUO06 calculated SM→ET as $(\Omega_E(S) - \Omega_E(W)) \cdot \sigma_E(W)$, where Ω_E is defined as in (A1) but for ET, and $\sigma_E(W)$ is the standard deviation of the 6-day average ET for the W runs. This definition considers two factors: a robust ET response to soil moisture ($\Omega_E(S) - \Omega_E(W)$) and
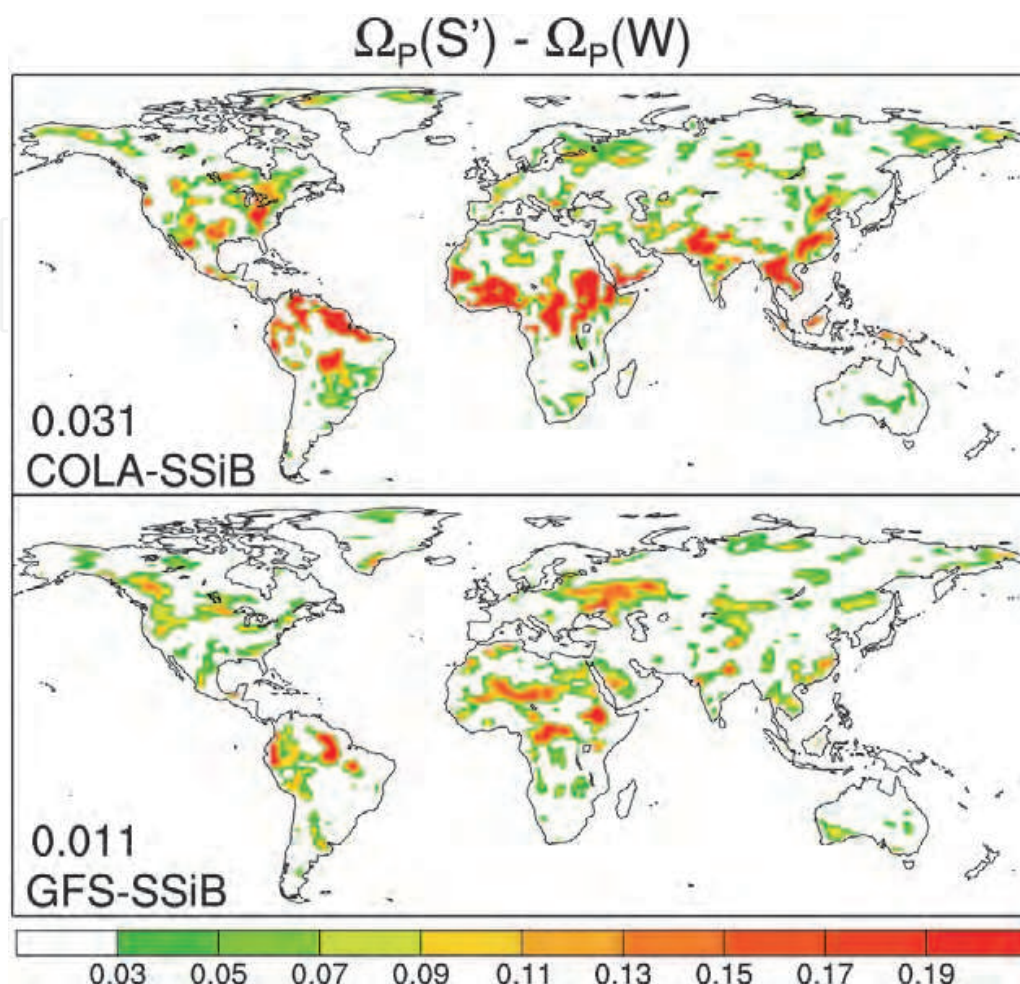
Fig. 4. Same as the right column of Fig. 1, but (top) the S runs of COLA-SSiB read soil moisture from a W run of GFS-SSiB, and (bottom) the S runs of GFS-SSiB read soil moisture from a W run of COLA-SSiB (from Wei and Dirmeyer 2010).

a high variability of ET ($\sigma_E(W)$). For soil moisture to have a strong impact on ET, both of them need to be sufficiently high. ET→P is simply calculated by GUO06 as the ratio of $\Omega_P(S) - \Omega_P(W)$ to SM→ET. (GUO06 introduced one more method for calculating ET→P, which produces similar results.) As mentioned, this diagnostic of SM→ET should be affected by the variability of precipitation and radiation. The experiment (2) above also demonstrates this indirectly. To verify this in another way, we calculate the inter-model correlation between ACR and SM→ET across the 12 GLACE models (Koster et al., 2006) (a correlation with a sample size of 12). We show results from GLACE models because we do not want our results to be limited to the models we use. It can be seen in Fig. 6a that there is substantial positive correlations between ACR and SM→ET over the globe, supporting our conjecture on the relationship between precipitation variability and SM→ET. The correlations between ACR and ET→P and between SM→ET and ET→P are both very low (Fig. 6b, 6c), suggesting that they are largely independent.
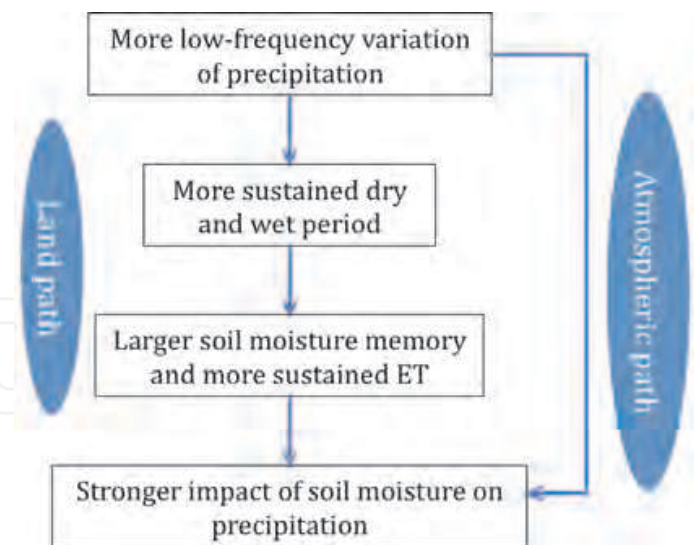
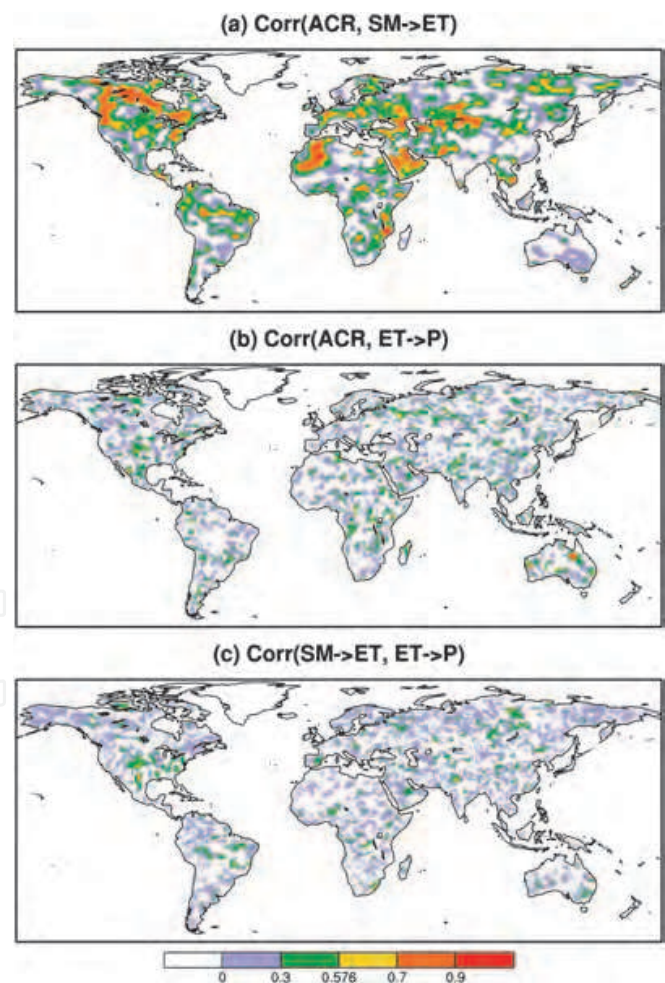Fig. 5. Schematic of the impact of precipitation variability on soil moisture-precipitation coupling.

Fig. 6. The correlations between (a) ACR and SM→ET, (b) ACR and ET→P, and (c) SM→ET and ET→P across the 12 models participating in GLACE. The values over 0.576 are significant at the 95% level (from Wei and Dirmeyer 2010).

6. Conceptual relationships

The above analysis shows that the spatial distribution of both $\Omega_P(W)$ and $\Omega_P(S)$ are largely consistent with that of the low-frequency variability of the atmosphere, which may come from the slow external forcing or internal atmospheric dynamics. We denote it as F. F can be measured by the percentage of IV or ACR, and we have shown above that ACR is a better metric. The conceptual relationship between Ω_p, F, and the impact of soil moisture α is given as

$$\Omega_p = F \cdot (\alpha_0 + \alpha) \tag{1}$$

where α_0 is a constant, and $\alpha_0 \gg \alpha$ over most regions. Thus, the spatial variation of Ω_p is largely determined by F, which is consistent with the analysis above. F is similar for both ensemble W and ensemble S, so the coupling strength

$$\Omega_p(S) - \Omega_p(W) = F \cdot (\alpha(S) - \alpha(W)), \tag{2}$$

where $\alpha(S) - \alpha(W)$ is the difference of α between the two ensembles and can be further expanded to SM→ET and ET→P. Therefore

$$\Omega_P(S) - \Omega_P(W) = F \cdot SM \rightarrow ET(F) \cdot ET \rightarrow P, \tag{3}$$

where SM→ET is a function of F and some other model parameterizations. All the three factors—F, SM→ET, and ET→P may impact the coupling strength. The impact of F is separated from that of SM→ET because the impact of the atmosphere can be independent of the land surface. This multiplicative form of the equation considers the nonlinear combination of the factors. When SST is prescribed, F is mainly a property of the AGCM, especially the convection scheme. SM→ET is affected by both the LSS and the AGCM, and ET→P is mainly determined by the AGCM, especially the convection and boundary layer parameterizations. This decomposition, although is still conceptual, integrates our current understanding on land-atmosphere coupling, and it makes diagnosing land-atmosphere coupling much easier.

GUO06 only partly considers the impact of F (through SM→ET) and attributes the rest of the coupling strength to ET→P. They found that, for the 12 GLACE models, SM→ET has stronger correlation with the coupling strength than ET→P, and concluded that SM→ET is the main cause of the differences in the coupling strength. However, we show that the differences in SM→ET can be partly attributed to the impact of atmospheric variability, so it is still hard to say whether the different AGCMs or the different LSSs is the main cause of the differences in coupling strength. In spite of that, for our six model configurations here, the multi-model coupling method has clearly shown that the difference between the AGCMs is the main reason. It remains possible that the differences among the three LSSs are unusually small or the differences between the two AGCMs are unusually large.

7. Calibration of the estimated GLACE land-atmosphere coupling strength

In order to examine whether our results on the overestimation of low-frequency variance and its relationship with Ω_p also apply to other models, we look at the GLACE dataset
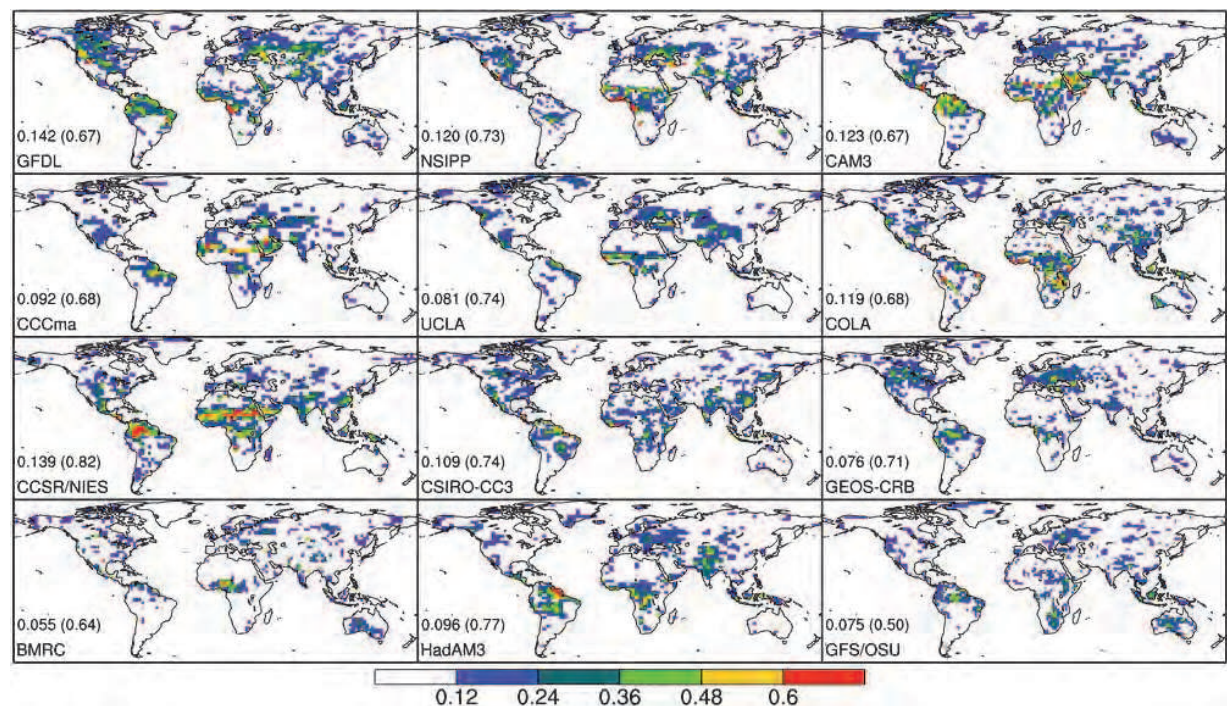
Fig. 7. Same as Fig. 3, but for the 12 models participating in GLACE (all from ensemble W; ensemble S has similar results). The first value at the left corner of each panel is the global mean (land only), and the second value (in the parentheses) is the spatial correlation of ACR with $\Omega_p(W)$.

(Koster et al. 2006). Fig. 7 shows the ACR for 12 models participating in the GLACE, and their respective spatial correlations with Ω_p. Similar to our model simulations above, ensemble S (not shown) shows very similar results to ensemble W. Also, all the models here have overestimated the mean ACR compared to the GPCP results, and their average is about double the ACR of GPCP (Fig. 8). The spatial correlations of ACR and Ω_p are always high; even the lowest value (0.5 from GFS/OSU) is well over the 99% confidence level (assume the grid points are independent). Therefore, the GLACE models and our models show similar relationships between Ω_p and ACR.

We have shown that the estimate of precipitation predictability caused by soil moisture ($\Omega_P(S) - \Omega_P(W)$) is closely related to the atmospheric low-frequency variability F but the models generally overestimate it. The influence of F on $\Omega_P(S) - \Omega_P(W)$ is obviously shown in equations (2) and (3). However, we cannot conclude that the land-atmosphere coupling strength estimated by GLACE is overestimated, because other important factors (SM→ET and ET→P) are still not observed at large scale. Nonetheless, we may assume that the other factors from the model ensemble are better than that of most individual models, and try to correct F to make $\Omega_P(S) - \Omega_P(W)$ possibly closer to reality. Roughly, we calibrate the average $\Omega_P(S) - \Omega_P(W)$ for the 12 models at each grid point (all interpolated to a common 2.5°×2.5° grid as GPCP data):

$$(\Omega_P(S) - \Omega_P(W))_{calibrated} = (\Omega_P(S) - \Omega_P(W)) \frac{ACR(\text{obs})}{ACR(\text{models})}, \tag{4}$$

where ACR(obs)/ACR(models) is the ratio of ACR for GPCP data and the average ACR for the 12 models. This method tries to correct F by scaling it with a ratio of observed and modeled precipitation ACR. The GPCP-1DD data is used as ground truth observations. The ACR is calculated from ensemble W instead of ensemble S because it corresponds more closely to the real world (soil moisture is interactive). Note that the precipitation time series also contains a slice of the seasonal cycle during JJA, which is consistent with GLACE analysis. The predictability from seasonal variation is also important, because not every model can produce an accurate seasonal cycle. This calibration method considers model biases in both intraseasonal and seasonal variances. If removing the predictability from the seasonal variation, the coupling strength will be weaker but the patterns are similar (not shown).
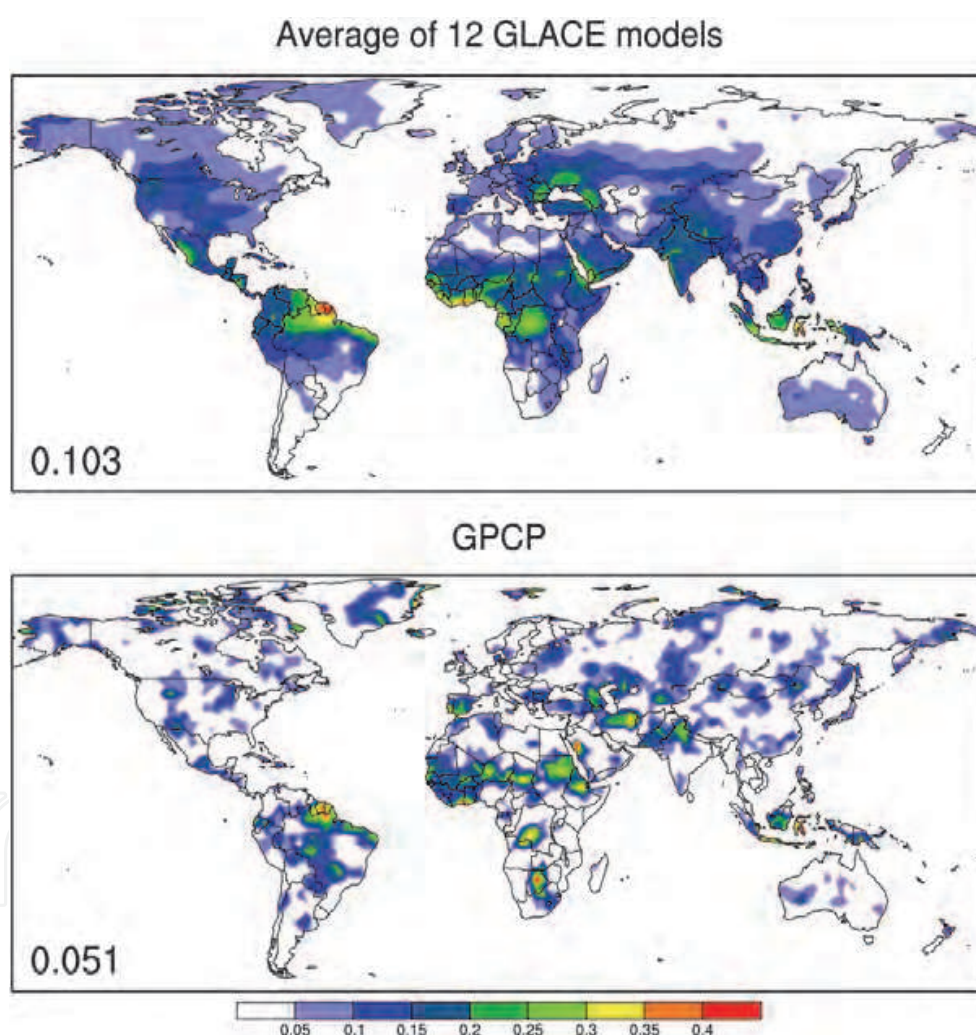

Fig. 8. Same as Fig. 3, but (top) for the average of 12 models participating in GLACE and (bottom) GPCP (same as in Fig. 3).

Although the spatial correlations between Ω_p and the ACR are very significant for all the models, the strong connection between Ω_p and F described in equation (1) may not happen over all the regions. The noise may damp the connection in some cases. We then calculated the correlation between Ω_p and ACR across the 12 GLACE models (a correlation with a

sample size of 12; Fig. 9). It indicates a general connection between Ω_p and ACR for all the 12 models at each grid point. The regions with strong positive correlation are where Ω_p and ACR have a strong connection for almost all the models. Over other regions where the correlation is positive but not so strong, their relationship may not be so consistent for the models but larger F can generally lead to larger Ω_p. We can see in Fig. 9 that over 95% of the land areas show positive correlations and more than half land areas show significant correlations (at 95% level), which supports our assumptions on their relationship.

Based on the above analysis, we perform a calibration over the regions where the correlation in Fig. 9 is over 95% confidence level (0.576), using equation (4). The results are shown in Fig. 10. It can be seen that the coupling strength reduces by about 20% after calibration, but global pattern is similar to the original one. The coupling strength is significantly weakened over US Great Plains, Mexico, and Nigeria. The pattern over India and Pakistan changes a little. In Wei et al. (2010b), we have preformed a similar calibration using the percentage of IV instead of ACR. The results are largely similar, but the coupling strength over US Great Plains weakened less.

Due to the changing and heterogeneous nature of the relationship between Ω_p and F, our calibration method is not flawless. However, the results illustrate how the amplitude and distribution of coupling strength may change after some rectification of the model bias. The unique design of GLACE makes its results difficult to evaluate by directly comparing them with observational variables, even if these large-scale observations exist, because the GLACE metric is based on ensemble statistics, and observations present us with only one "ensemble member". Some recent studies using observational based data have cast doubt on the strong coupling strength in the Great Plains (Ruiz-Barradas and Nigam 2005, 2006; Zhang et al. 2008), but whether their results are comparable to the GLACE result need further study. On the other hand, Wang et al. (2007) have shown that less restrictive metrics than measuring ensemble coherence, such as the change in overall precipitation variance between S and W cases, reveals even more areas of apparently strong coupling strength.
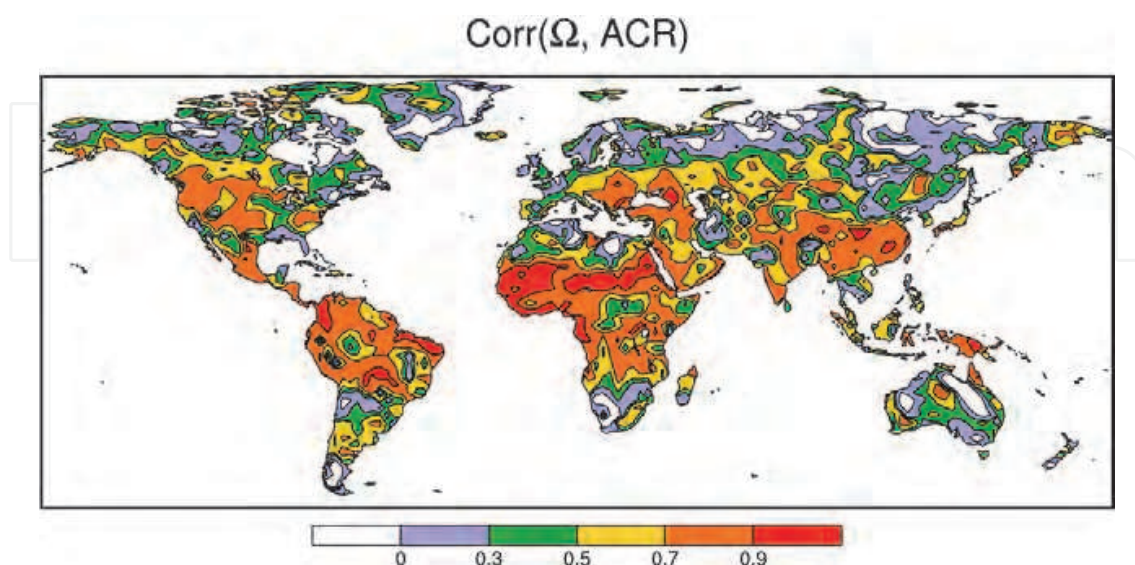

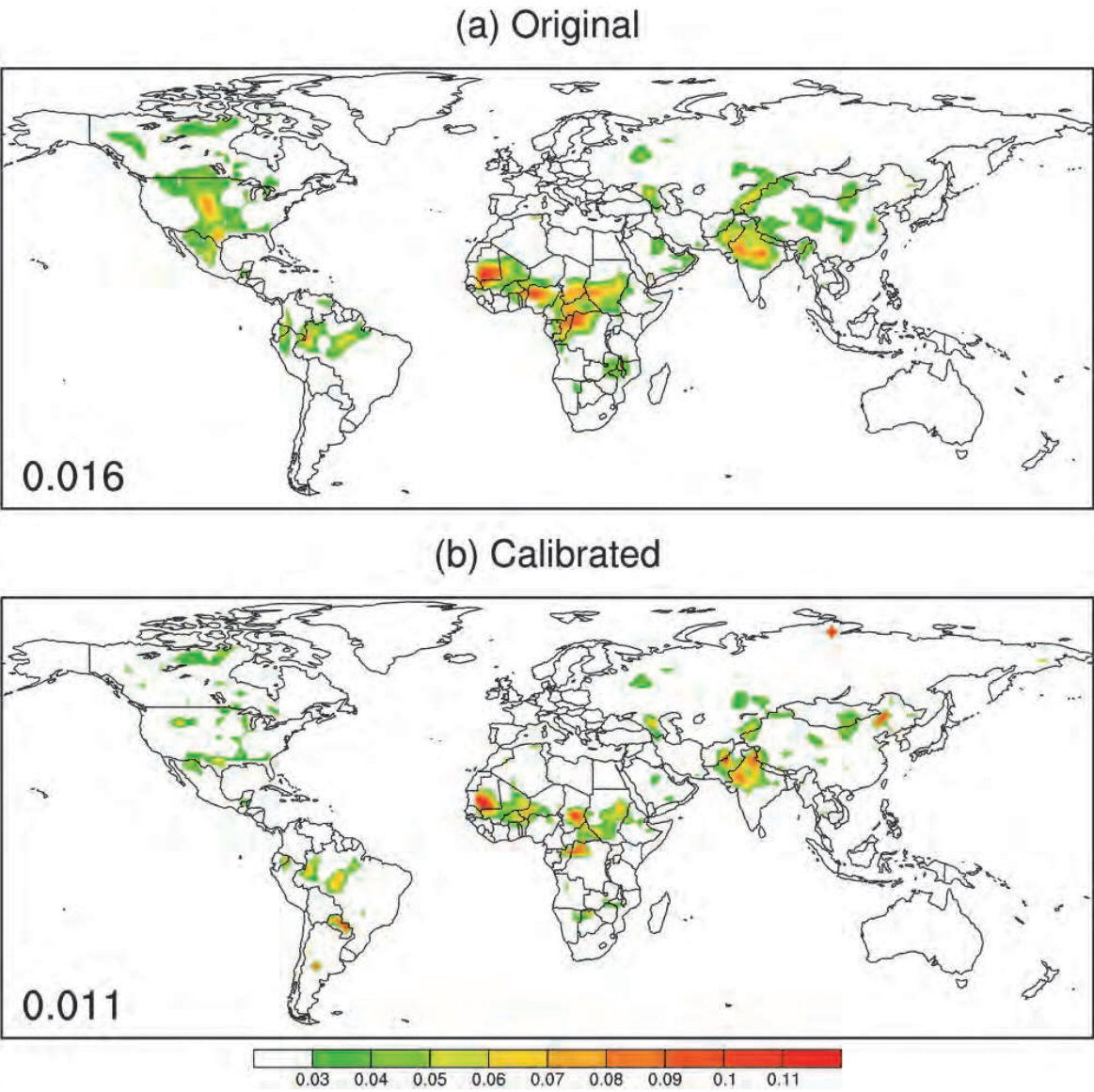Fig. 9. The correlation between $\Omega_P(W)$ and ACR across the 12 models participating in GLACE.

Fig. 10. The estimated land-atmosphere coupling strength ($\Omega_P(S) - \Omega_P(W)$). (a) From the original GLACE dataset. (b) Calibrated result. Only the regions where correlation in Fig. 8 exceeds 0.576 (95% confidence level) are calibrated. The global average value is shown at the left corner of each panel.

8. Conclusions and discussion

Coupling one AGCM to three different land models gives us an unprecedented opportunity to study the role of different components in land-atmosphere interaction. The behavior of the coupled models and their land-atmosphere interaction are investigated by a set of GLACE-type experiments. It is found that the two AGCMs determine the overall spatial distribution and amplitude of precipitation variability, predictability, and land-atmosphere coupling for the six model configurations. The impact of different LSSs is mostly regional. Different LSSs or soil moisture have little influence on the global pattern of precipitation predictability and variance distribution because of the stronger control of other factors. The estimated precipitation predictability and land-atmosphere coupling strength is closely

related to the low-frequency variability of atmosphere, which can impact land-atmosphere coupling both directly in the atmosphere and indirectly through soil moisture response to precipitation. Based on these findings, the land-atmosphere coupling strength is conceptually decomposed into the impact of low-frequency precipitation variability, the impact of soil moisture on evapotranspiration (ET), and the impact of ET on precipitation. As most models participating in GLACE have overestimated the low-frequency component of precipitation, a rough calibration to the GLACE-estimated land-atmosphere coupling strength is performed. The calibrated coupling strength shows a similar global pattern, but is significantly weaker over some regions, like US Great Plains and Mexico.

We discussed the land-atmosphere coupling strength based on the index defined in GLACE, which emphasizes the temporal coherency of the precipitation time series among the ensemble members. Analysis with another index defined by Wang et al. (2007), which emphasizes the relative divergence of mean precipitation, does not show significant overall differences in the coupling strength between GFS and COLA AGCM configurations. This suggests the important role of atmospheric variability in determining the different GLACE coupling strengths of GFS and COLA AGCM configurations.

The integration period of these GLACE-type experiments is JJA, so the longest timescale in this study is intraseasonal. The effect of land may be different for longer timescales. Our judgment on the connections between external forcing, low-frequency precipitation variability, and Ω_p and $\Omega_P(S) - \Omega_P(W)$ is based on model results so may not be absolutely true in reality. Some intraseasonal variations of precipitation may not come from external forcing but from the flow instabilities (especially in midlatitudes; e.g., Charney and Shukla 1981) that are not fully understood nor properly simulated. The observational datasets used in this study are all based on satellite observations, and they may have consistent biases. In spite of these limitations, this study qualitatively separates the role of external forcing and local soil moisture on precipitation variability and predictability, and increases our understanding of land-atmosphere interaction.

9. Appendix

9.1 Global Land-Atmosphere Coupling Experiment (GLACE)

GLACE (Koster et al. 2004, 2006) is a model inter-comparison study focusing on evaluation of the role of land state in numerical weather and climate predictions. It consists of sets of 16-member ensembles of AGCM experiment (we only discuss two sets here). Ensemble W as a set of free runs with different initial land and atmosphere conditions but forced by the same SST from 1994, and ensemble S is the same as ensemble W except that, at each time step, the soil moisture in all the soil layers is replaced by that from one member chosen from ensemble W (all members of S have the same soil moisture). This is a little different from that of the standard GLACE experiments, where only subsurface soil moisture was replaced in the S ensemble. We design the experiments in this way to make the results from different LSSs more comparable; it has been shown that the upper layer of Noah model is responsible for an unusually large part of evapotranspiration (Zhang et al. 2010). All runs cover the period of 1 June-31 August, 1994. A diagnostic variable Ω was defined in GLACE:

$$\Omega = \frac{16\sigma^2_{<X>} - \sigma^2_X}{15\sigma^2_X} , \tag{A1}$$

where σ^2_X is the intraensemble variance of variable X, and $\sigma^2_{<X>}$ is the corresponding variance of ensemble mean time series. In calculating the variance, the first 8 days of data of each run is discarded to avoid model initial shock, and the remaining 84 days are aggregated into 14 six-day totals. Therefore, σ^2_X is a variance across 224 (16×14) six-day totals from all the ensemble members, and $\sigma^2_{<X>}$ is a variance across 14 six-day totals from the ensemble mean time series.

Theoretically, if the 16 members of an ensemble have identical time series of X, $\sigma^2_{<X>}$ will be equal to σ^2_X and Ω will be 1; if the X time series of the 16 members are completely independent, $\sigma^2_{<X>}$ will be equal to $\sigma^2_X / 16$ and Ω will be 0. Without sampling error, Ω will range between 0 and 1. Ω measures the similarity (or predictability) of the time series in 16 ensemble members. Analyses show that Ω emphasizes the temporal coherency, or the phase relationship, more than the mean and temporal variance of the time series (Wang et al. 2007; Yamada et al. 2007). Mathematically, Ω is equivalent to the percentage of variance caused by the slowly varying oceanic, radiative, and land surface processes (Koster et al. 2006; Yamada et al. 2007). The difference of Ω from the two ensembles, $\Omega(S) - \Omega(W)$, is then equivalent to the percentage of variance caused by the prescribed soil moisture, and is a measure of land-atmosphere coupling strength in GLACE.
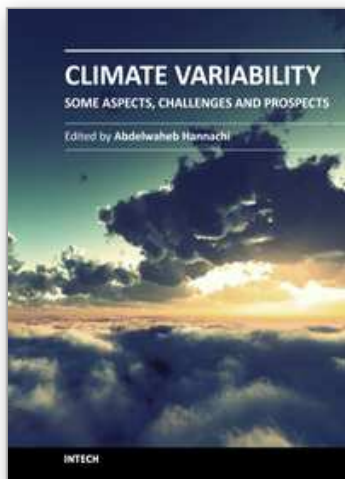
10. Acknowledgement

11. References

Charney, J. G. and J. Shukla, 1981: Predictability of monsoons. Monsoon Dynamics, Editors: Sir James Lighthill and R. P. Pearce, Cambridge University Press, pp. 99-109.

Delworth, Thomas, Syukuro Manabe, 1989: The Influence of Soil Wetness on Near-Surface Atmospheric Variability. J. Climate, 2, 1447–1462.

Dirmeyer, P. A., 2006: The hydrologic feedback pathway for land-climate coupling. J. Hydrometeor., 7, 857-867.

Dirmeyer, P. A., and F. J. Zeng, 1999: An update to the distribution and treatment of vegetation and soil properties in SSiB. COLA Technical Report 78, Center for Ocean-Land-Atmosphere Studies, Calverton, MD, 27 pp.

Dirmeyer, P. A., R. D. Koster, and Z. Guo, 2006: Do global models properly represent the feedback between land and atmosphere? J. Hydrometeor., 7:1177–1198.

Dirmeyer, P. A., Z. Guo, and J. Wei, 2010: Building the case for (or against) land-driven climate predictability. iLEAPS Newsletter. No. 9, 14-17.

Dirmeyer, P.A., M.J. Fennessy, and L. Marx, 2003: Low Skill in Dynamical Prediction of Boreal Summer Climate: Grounds for Looking beyond Sea Surface Temperature. J. Climate, 16, 995–1002.

Ek, M. B., and Coauthors, 2003: Implementation of Noah land surface model advances in the National Centers for Environmental Prediction operational mesoscale Eta model, J. Geophys. Res., 108(D22), 8851, doi:10.1029/2002JD003296.

Gao, X. and P. A. Dirmeyer, 2006: A multimodel analysis, validation, and transferability study of global soil wetness products. J. Hydrometeor., 7:1218–1236.

Graham, N.E., T.P. Barnett, R. Wilde, M. Ponater, and S. Schubert, 1994: On the Roles of Tropical and Midlatitude SSTs in Forcing Interannual to Interdecadal Variability in the Winter Northern Hemisphere Circulation. J. Climate, 7, 1416–1441.

Guo, Z., and Coauthors, 2006: GLACE: The Global Land–Atmosphere Coupling Experiment. Part II: Analysis. J. Hydrometeor., 7, 611–625.

Guo, Z., P. A. Dirmeyer, X. Gao, and M. Zhao, 2007: Improving the quality of simulated soil moisture with a multi-model ensemble approach. Quart J.Roy. Meteor. Soc., 133, 731-747.

Huffman, G.J., R.F. Adler, M. Morrissey, D.T. Bolvin, S. Curtis, R. Joyce, B McGavock, J. Susskind, 2001: Global Precipitation at One-Degree Daily Resolution from Multi-Satellite Observations. J. Hydrometeorol., 2, 36-50.

Joyce, R. J., J. E. Janowiak, P. A. Arkin, and P. Xie, 2004: CMORPH: A method that produces global precipitation estimates from passive microwave and infrared data at high spatial and temporal resolution. J. Hydrometeorol., 5, 487-503.

Kinter J. L., and Coauthors, 1997: The COLA atmosphere-biosphere general circulation model. Vol. 1: Formulation. COLA Tech. Rep. 51, 46 pp. Center for Ocean–Land–Atmosphere Studies, Calverton, MD.

Koster R. D. and Suarez M. J., 1995: Relative contributions of land and ocean processes to precipitation variability. Journal of Geophysical Research 100, 13775–13790.

Koster, R. D., and Coauthors 2004: Regions of strong coupling between soil moisture and precipitation, Science, 305, 1138-1140.

Koster, R. D., and Coauthors, 2006: GLACE: The Global Land-Atmosphere Coupling Experiment. Part I: Overview, J. Hydrometeorol., 7, 590–610.

Koster, R.D., M.J. Suarez, and M. Heiser, 2000: Variance and Predictability of Precipitation at Seasonal-to-Interannual Timescales. J. Hydrometeor., 1, 26–46.

McPhee, J., and S.A. Margulis, 2005: Validation and Error Characterization of the GPCP-1DD Precipitation Product over the Contiguous United States. J. Hydrometeor., 6, 441–459.

Misra, V., and Coauthors, 2007: Validating and understanding ENSO simulation in two coupled climate models, Tellus, Ser. A, 59, 292–308.

Pitman, A. J. 2003: The evolution of, and revolution in, land surface schemes designed for climate models, Int. J. Climatol., 23, 479-510.

Quan, X.W., P.J. Webster, A.M. Moore, and H.R. Chang, 2004: Seasonality in SST-Forced Atmospheric Short-Term Climate Predictability. J. Climate, 17, 3090–3108.

Ruane, A. C., and J. O. Roads, 2008: Diurnal to Annual Precipitation Sensitivity to Convective and Land Surface Schemes. Earth Interactions, 12, 1–13.

Ruane, A.C., and J.O. Roads, 2007: 6-Hour to 1-Year Variance of Five Global Precipitation Sets. Earth Interactions, 11, 1–29.

Ruiz-Barradas, A., and S. Nigam, 2005: Warm Season Rainfall Variability over the U.S. Great Plains in Observations, NCEP and ERA-40 Reanalyses, and NCAR and NASA Atmospheric Model Simulations. J. Climate, 18, 1808–1830.

Ruiz-Barradas, A., and S. Nigam, 2006: Great Plains Hydroclimate Variability: The View from North American Regional Reanalysis. J. Climate, 19, 3004–3010.

Shukla J., and Coauthors 2000: Dynamical seasonal prediction. Bull. Amer. Meteor. Soc., 81, 2593–2606.

Shukla, J. 1993: Predictability of short-term climate variations. Prediction of Interannual Climate Variations. NATO ASI Series I: Global Environmental Change, Vol. 6, Editor: J. Shukla, 217-232.

Shukla, J. 1998: Predictability in the midst of Chaos: A scientific basis for climate forecasting. Science, 282, 728-731.

Su, F., Y. Hong, and D.P. Lettenmaier, 2008: Evaluation of TRMM Multisatellite Precipitation Analysis (TMPA) and Its Utility in Hydrologic Prediction in the La Plata Basin. J. Hydrometeor., 9, 622–640.

Sun, Y., S. Solomon, A. Dai, and R.W. Portmann, 2006: How Often Does It Rain? J. Climate, 19, 916–934.

Trenberth, K. E., A. Dai, R. M. Rasmussen, and D. B. Parsons, 2003: The Changing Character of Precipitation. *Bull. Amer. Meteor. Soc.*, 84, 1205–1217.

Wang, G., Y. Kim and D. Wang, 2007: Quantifying the strength of soil moisture-precipitation coupling and its sensitivity to changes in surface water budget. J. Hydrometeor., 8, 551-570.

Wei, J. and P. A. Dirmeyer, 2010: Toward understanding the large-scale land-atmosphere coupling in the models: Roles of different processes, Geophys. Res. Lett., 37, L19707, doi:10.1029/2010GL044769.

Wei, J., P. A. Dirmeyer, and Z. Guo, 2010b: How much do different land models matter for climate simulation? Part II: A decomposed view of land-atmosphere coupling strength. J. Climate. 23, 3135-3145.

Wei, J., P. A. Dirmeyer, Z. Guo, L. Zhang, and V. Misra, 2010a: How much do different land models matter for climate simulation? Part I: Climatology and variability. J. Climate. 23, 3120-3134.

Wei, J., R. E. Dickinson, and N. Zeng, 2006: Climate variability in a simple model of warm climate land-atmosphere interaction, J. Geophys. Res., 111, G03009, doi:10.1029/2005JG000096.

Wei, J., R.E. Dickinson, and H. Chen, 2008: A Negative Soil Moisture–Precipitation Relationship and Its Causes. J. Hydrometeor., 9, 1364–1376.

Wilcox, E.M., and L.J. Donner, 2007: The Frequency of Extreme Rain Events in Satellite Rain-Rate Estimates and an Atmospheric General Circulation Model. J. Climate, 20, 53–69.

Xie, P., J.E. Janowiak, P.A. Arkin, R. Adler, A. Gruber, R. Ferraro, G.J. Huffman, and S. Curtis, 2003: GPCP Pentad Precipitation Analyses: An Experimental Dataset Based on Gauge Observations and Satellite Estimates. J. Climate, 16, 2197–2214.

Xue, Y., P. J. Sellers, J. L. Kinter, J. Shukla, 1991: A simplified biosphere model for global climate studies, J. Climate, 4, 345-364.

Yamada, T.J., R.D. Koster, S. Kanae, and T. Oki, 2007: Estimation of Predictability with a Newly Derived Index to Quantify Similarity among Ensemble Members. Mon. Wea. Rev., 135, 2674–2687.

Zhang, J., W.-C. Wang, and J. Wei, 2008: Assessing land-atmosphere coupling using soil moisture from the Global Land Data Assimilation System and observational precipitation, J. Geophys. Res., 113, D17119, doi:10.1029/2008JD009807.

Zhang, L., P. A. Dirmeyer, J. Wei, Z. Guo and C.-H. Lu, 2011: Land-atmosphere Coupling Strength in the Global Forecast System. J. Hydrometeor., 12, 147–156.

Climate Variability - Some Aspects, Challenges and Prospects

Edited by Dr. Abdel Hannachi

This book provides a general introduction to the popular topic of climate variability. It explores various aspects of climate variability and change from different perspectives, ranging from the basic nature of low-frequency atmospheric variability to the adaptation to climate variability and change. This easy and accessible book can be used by professionals and non professionals alike.

How to reference

In order to correctly reference this scholarly work, feel free to copy and paste the following:

Jiangfeng Wei, Paul A. Dirmeyer, Zhichang Guo and Li Zhang (2012). Impact of Atmospheric Variability on Soil Moisture-Precipitation Coupling, Climate Variability - Some Aspects, Challenges and Prospects, Dr. Abdel Hannachi (Ed.), ISBN: 978-953-307-699-7, InTech, Available from: http://www.intechopen.com/books/climate-variability-some-aspects-challenges-and-prospects/impact-of-atmospheric-variability-on-soil-moisture-precipitation-coupling

INTECH

open science | open minds